Nonmonotonic relaxation kinetics of confined systems

Yaroslav E. Ryabov, Alexander Puzenko, and Yuri Feldman*
Department of Applied Physics, The Hebrew University of Jerusalem, Givat Ram, 91904, Jerusalem, Israel
(Received 2 September 2003; published 14 January 2004)

The specific features of relaxation kinetics in systems with different kinds of confinements are discussed in the paper. In contrast to the usual Arrhenius, Eyring, or Vogel-Fulcher-Tammann patterns, a quite unusual nonmonotonic dependence of relaxation time versus temperature is observed in such systems. Based on the free volume concept, a model for this type of kinetics was illustrated by several particular examples: water confined in porous glasses and in zeolites, confined liquid crystals, doped ferroelectric crystals, and heteropolymer folding.

DOI: 10.1103/PhysRevB.69.014204 PACS number(s): 61.20.Lc, 77.22.Gm, 87.15.Cc

INTRODUCTION

Historically the term *kinetics* was introduced in chemistry for the temperature dependency of chemical reaction rates. The simplest model, which describes the dependency of reaction rate k on temperature T, is the so-called Arrhenius law,[1]

$$k = k_0 \exp\left(-\frac{E_a}{k_B T}\right), \tag{1}$$

where E_a is activation energy, $k_B = 1.381 \times 10^{-23}$ J K^{-1} is the Boltzmann constant, and k_0 is the pre exponential factor corresponding to the fastest reaction rate at the limit $T \to \infty$. In his original paper[1] Arrhenius deduced this kinetic law from the transition state theory. The basic idea behind Eq. (1) was considered to be the single-particle process provided by the transition between two states separated by the potential barrier of height E_a. After Arrhenius, many authors suggested several other explanations for Eq. (1) and proposed similar models, which described chemical reaction kinetics.[2] Then the next development of the chemical reaction rates theory was provided by Eyring,[2–4] who suggested a more advanced model:

$$k = \frac{k_B T}{\hbar} \exp\left(\frac{\Delta S}{k_B} - \frac{\Delta H}{k_B T}\right), \tag{2}$$

where ΔS is activation entropy, ΔH is activation enthalpy, and $\hbar = 6.626 \times 10^{-34}$ J s is the Plank constant. As in the case of Eq. (1) the Eyring law (2) is also based on the idea of a transition state. However, in contrast to the Arrhenius model (1), the Eyring Eq. (2) is based on more accurate evaluations for the equilibrium reaction rate constant, producing the extra factor proportional to the temperature.

The models (1) and (2) are used to explain the kinetics of chemical reaction rates and were also found to be very useful for other applications. Taking into account the relationship $\tau \sim 1/k$, Eqs. (1) and (2) can describe the temperature dependency of relaxation time τ versus temperature for the processes such as dielectric or mechanical relaxation that are not related to chemical transmutations. The reason for this similarity is the idea of a transition state for a chemical reaction that considers the energy barrier between the initial and final state. Therefore, relaxation processes, provided by the transition between the two states separated by an energy barrier, may also obey Arrhenius or Eyring laws. In this paper we shall discuss the temperature dependencies of relaxation times and argue about such processes as for the ''relaxation kinetics.''

The relaxation kinetics of Arrhenius and Eyring types were found for an extremely wide class of systems in different aggregative states.[5–8] Nevertheless, in many cases, these laws cannot explain the experimentally observed temperature dependences of relaxation rates in different systems. Thus, to describe the relaxation kinetic, especially for amorphous and glass-forming substances,[9–13] many authors have used the following expression:

$$\ln\left(\frac{\tau}{\tau_0}\right) = \frac{D T_K}{T - T_K}, \tag{3}$$

where T_K is the characteristic temperature at which the relaxation time diverges and D is the dimensionless constant widely referred to as fragility. This model was first proposed in 1921 by Vogel.[14] Shortly after it was independently discovered by Fulcher[15] and then utilized by Tammann and Hesse[16] to describe their viscosimetric experiments. Thus, Eq. (3) has been referred to as the Vogel-Fulcher-Tammann (VFT) law. It is widely held now that VFT relaxation kinetics found its explanation in the framework of the Adam and Gibbs model.[17] This model is based on the Kauzmann concept of configurational entropy,[12,18] which is supposed to disappear for an amorphous substance at temperature T_K. Thus, based on this configurational entropy concept, the coincidence between the experimental data and VFT law is usually interpreted as a sign of cooperative behavior in a disordered-glass-like state.

An alternative explanation of the VFT model (3) is based on the free volume concept introduced by Fox and Floury[19–21] to describe the relaxation kinetics of polystyrene. The main statement of this concept is that the probability of moving a polymer molecule segment is related to the free volume availability in a system. Later the concept of free volume was applied to the wider class of disordered solids by Doolittle[22] and Turnbull and Cohen,[23] who suggested similar relationships that in the terms of relaxation times could be rewritten in the form

$$\ln\left(\frac{\tau}{\tau_0}\right)=\frac{v_0}{v_f}, \tag{4}$$

where v_0 is the volume of a molecule (a mobile unit) and v_f is the free volume per molecule (per mobile unit). Thus, if one implies that the free volume increases with temperature $v_f \sim T-T_K$, then from Eq. (4) the VFT law (3) is immediately obtained.

Later, the VFT kinetic model was generalized by Bendler and Shlesinger.[24] Starting from the assumption that the relaxation of an amorphous solid is provided by some mobile defects, they deduced the relationship between τ and T in the form

$$\ln\left(\frac{\tau}{\tau_0}\right)=\frac{B}{(T-T_K)^{3/2}}, \tag{5}$$

where B is a constant dependent on the defect concentration and the characteristic correlation length of the defect space distribution.[24] The model (5) is not as popular as the VFT law; however, it has been found to be really useful for some particular substances.[25,26]

Another type of currently discussed kinetics pattern is related to the so-called mode-coupling theory (MCT) developed by Götze and Sjögren,[27] which suggests that the cooperative relaxation process in supercooled liquids and amorphous solids is a kind of a critical phenomenon and predicts the dependency of relaxation time versus temperature for such substances in the form

$$\tau \sim (T-T_c)^{-\gamma}, \tag{6}$$

where T_c is a critical temperature and γ is the critical MCT exponent. Equation (6) was introduced for the first time by Bengtzelius *et al.*[28] to discuss the temperature dependency of viscosity for methyl-cyclopean and later was utilized for a number of other systems.[29,30]

The short review of different models for the relaxation kinetics presented above cannot possibly cover all known possibilities. However, as can be seen from Eqs. (1)–(3), (5), and (6), the vast majority of relaxation kinetics models implies a monotonic decrease of relaxation time with an increase in temperature. Nevertheless, recently the scientific community has witnessed several absolutely different experimental observations of nonmonotonic relaxation kinetics.[31–41] In the present work we are going to discuss the possible reasons for such nonmonotonic relaxation kinetics, using several different examples borrowed from recent experimental studies.

It seems that the first experimental example of the nonmonotonic relaxation kinetics was observed by Schöler *et al.* in Ref. 31 on the dielectric relaxation of glass-forming liquid *N*-methyl-caprolactam confined in porous glass (see Fig. 1b in Ref. 31). In that work this relaxation process was attributed to the Maxwell-Wagner-Sillars (MWS) interfacial polarization effect. However, the experimental data presented there[31] do not clearly show the reverse of the relaxation time temperature dependence. Thus, to the best of our knowledge, the dielectric relaxation study[32] of water confined in porous glasses was the first work in which the nonmonotonic temperature dependence of τ was clearly demonstrated and assigned to the specific relaxation process. In this case, the usual decrease of the relaxation time with increase in temperature in the low temperature region could be observed, while in the high temperature region a further temperature increase leads to the reverse of this tendency (see Fig. 1 in Ref. 32). At that time the reasons for this kinetics pattern were baffling and the authors of Ref. 32 analyzed only the low temperature part of the saddlelike Arrhenius plot in the terms of VFT law (see Fig. 4 in Ref. 32).

Then, Frunza *et al.* observed[34] a similar saddlelike dependence of the relaxation time on temperature in the dielectric relaxation study of $Na_{58}(AlO_2)_{58}(SiO_2)_{136}\cdot mH_2O$ zeolite (NaY) of the faujasite type (see Fig. 4 in Ref. 34). Later in Ref. 35, similar to Refs. 32 and 33, this process was assigned to the relaxation of water molecules confined into the molecular cages of NaY.

Almost at the same time, nonmonotonic relaxation kinetics was mentioned by Aliev *et al.*[36] for the 4-*n*-*octyl*-4′-cyanobiphenyl (8CB) liquid crystal confined in oriented parallel cylindrical pores. In this case, the temperature dependency of the librational mode relaxation time for 8CB exhibits saddlelike behavior, as presented in Fig. 5 in Ref. 36.

Then, absolutely unexpectedly, the nonmonotonic dependence of the relaxation time on temperature was observed in a dielectric study of copper doped $KTa_{0.65}Nb_{0.35}O_3$ (KTN) ferroelectric crystal[37] of perovskite structure. In this case, the saddlelike process was observed in the ferroelectric phase of KTN and ascribed to the specific relaxation process related to the mobility of Cu ions.

It is curious to note that the folding kinetics of proteins[38,39] and heteropolymers[40] also show a saddlelike temperature dependence of folding time. In this work we shall discuss two particular examples of this behavior: the folding kinetics of chymotrypsin inhibitor 2 (CI2) (Ref. 39) and computer simulations of the random amino acids folding dynamics.[40] In the case of proteins and heteropolymers, this kinetic pattern is usually explained in the framework of the random energy model (REM) or by using a modification for the transition state theory.[38–40] However, as was demonstrated in Ref. 41, this process can also be discussed based on the idea of constraint in configurational space of the macromolecule conformations. In this paper all the situations mentioned above, excluding the first example from Ref. 31, are discussed in the framework of a single model.

THE MODEL

The model we are going to utilize here was first introduced to describe the relaxation properties of water adsorbed on the inner surfaces of porous glasses.[33] The main idea of this model is that the relaxation kinetics provided in this case by a process that needs to satisfy two statistically independent conditions. Thus, if one assigns the probability p_1 to satisfy the first condition and p_2 to satisfy the second condition, then the probability p to perform a relaxation act for such a system is

$$p=p_1p_2. \tag{7}$$

Let us discuss a system that consists of a number of particles where relaxation is provided by the reorientations (a jump or another type of transition) of particles between two local equilibrium states. In the spirit of the Arrhenius model, the first requirement for the relaxation is that the particles have enough energy to overcome the potential barrier E_a between the states of local equilibrium for elementary constituents of the system under consideration. Thus,

$$p_1 = \exp\left(-\frac{E_a}{k_B T}\right). \tag{8}$$

The essential idea of the model is that p_2 is the probability that there will be enough free volume in the vicinity of a relaxing particle to perform a reorientation. Then,

$$p_2 = \exp\left(-\frac{v_0}{v_f}\right). \tag{9}$$

By itself this probability represents a kind of constraint for the entire relaxation process and slows down the relaxation. Combining Eqs. (7)–(9) and taking into account the relationship $\tau \sim 1/p$, the following expression can obtained:

$$\ln\left(\frac{\tau}{\tau_0}\right) = \frac{E_a}{k_B T} + \frac{v_0}{v_f}. \tag{10}$$

As mentioned earlier it is usually assumed that the free volume grows with an increase in temperature. This idea reflects thermal expansion, i.e., if the number or relaxing particles in the system is kept constant, then the thermal expansion leads to an increase of the free volume with temperature growth. However, this concern may be wrong for the confined system in which the total volume is kept constant, but the number of relaxing particles varies. In this case, if one implies that the number n of relaxing particles obeys the Boltzmann law $n = n_0 \exp(-E_b/k_B T)$, then instead of Eq. (10) one immediately obtains[33]

$$\ln\left(\frac{\tau}{\tau_0}\right) = \frac{E_a}{k_B T} + C \exp\left(-\frac{E_b}{k_B T}\right), \tag{11}$$

where E_b is the energy required to make an inert particle participate in relaxation (or alternatively the energy required to form a so-called ''defect''), $C = v_0 n_0 / V$, and V is the total volume of the system. In contrast to all other considered kinetics models, Eq. (11) exhibits a nonmonotonic temperature dependency since it is related to two processes of a different nature: the Arrhenius term, reflecting the activated character of the relaxation process, and the exponential term, reflecting a decrease of the free volume per relaxing particle with increase in temperature. This second term is a consequence of constant volume constraint and the implication that the number of relaxing particles obeys Boltzmann law. If the total volume of the system V is sufficiently large and the maximum possible concentration of relaxing particles is sufficiently small $n_0/V \ll 1/v_0$, then the free volume arguments become irrelevant and relaxation kinetics obtains an Arrhenius form. However, in the case of a constraint, when the volume of a system is small and $n_0/V \approx 1/v_0$, an increase of temperature leads to a significant decrease of free volume and slows down the relaxation. As we are going to show, this situation usually occurs for ''small'' systems where relaxing particles become able to participate in the relaxation due to the formation of some ''defects'' in ordered structure. In this case n_0 could be regarded as the maximum possible defect concentration. Therefore, confinement provides a comparatively large concentration of defects n_0/V, since for such a system the confining geometry affects a comparatively larger amount of system constituents.

A quite straightforward consequence of Eq. (11) is that this relaxation kinetics reaches the shortest relaxation time τ_{fast},

$$\tau_{fast} = \tau_0 \left(eC\frac{E_b}{E_a}\right)^{E_a/E_b}, \tag{12}$$

at the optimal temperature T_{opt},

$$T_{opt} = \frac{E_b}{k_B \ln(C E_b / E_a)}, \tag{13}$$

where $e \approx 2.718$ is the base of natural logarithm. From Eqs. (12) and (13) it follows that the confinement is really important for this process. For example, if the total volume of system V decreases, then, under all other equal conditions, a longer value of τ_{fast} occurs at lower T_{opt}.

EXAMPLES

Dielectric relaxation of confined water

The present paper discusses two experimental examples related to the dielectric spectroscopy of water confined at the inner interface of porous glasses[32,33] and in the NaY zeolite $[Na_{58}(AlO_2)_{58}(SiO_2)_{136} \cdot m H_2O]$.[34,35] It is known[6,42] that the dielectric relaxation of water is due to a reorientation of water molecules that have a permanent dipole moment (6×10^{-30} C m or 1.8 D). It is also known[6,42] that in bulk water and ice, water molecules are embedded in the network structure of hydrogen bonds. Thus, the reorientation of a water molecule, leading to the dielectric relaxation, may occur only in the vicinity of a defect in the hydrogen bond network structure. A similar mechanism for confined water relaxation was proposed recently.[33] In this case, E_a can be regarded as the activation energy of reorientation of a water molecule and E_b as the defect formation energy.

Figures 1 and 2 present the experimental data for the dielectric relaxation of water confined in the porous glasses and zeolite, respectively. Figure 1 shows one can find three curves corresponding to the three different porous glasses samples A, B, and C that are different in their structure (average pore diameter) and chemical treatment. Figure 2 represents two different experimental runs for the same NaY zeolite sample. The fitting curves presented in these figures show that the model (11) is in good agreement with the experimental data. The fitted values of E_a and E_b for all the samples are in fair agreement with the energies attributed to the water molecule reorientation and defect formation for the bulk ice I that are evaluated as 55.5 kJ/mol and 32.9 kJ/mol, respectively.[6,42] This fact leads to the conclusion that most

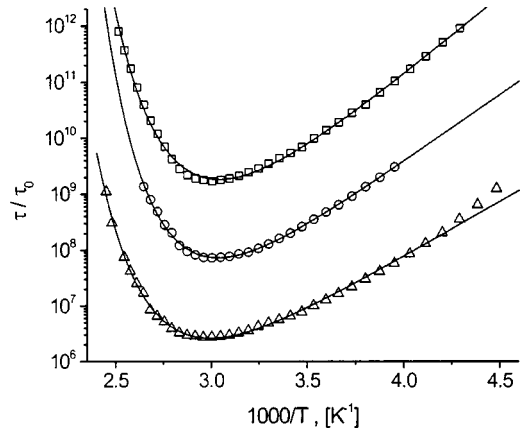

FIG. 1. Temperature dependency of the dielectric relaxation time of water confined in porous glasses (Ref. 33). Symbols represent experimental data. Full lines correspond to the best fit according to Eq. (11). Sample A (cycles): $\ln \tau_0 = -27 \pm 0.5$, $E_a = 46 \pm 1$ kJ/mol, $E_b = 33 \pm 1$ kJ/mol, $C = 27 \times 10^4 \pm 9 \times 10^4$. Sample B (boxes): $\ln \tau_0 = -33 \pm 0.5$, $E_a = 53 \pm 1$ kJ/mol, $E_b = 29 \pm 1$ kJ/mol, $C = 7 \times 10^4 \pm 2 \times 10^4$. Sample C (triangles): $\ln \tau_0 = -26 \pm 0.3$, $E_a = 38 \pm 1$ kJ/mol, $E_b = 32 \pm 1$ kJ/mol, $C = 12 \times 10^4 \pm 3 \times 10^4$.

probably the water confined in small pores is quite immobile and represents a kind of icelike structure. For further discussion more detailed information about the samples should be recalled. For example, let us discuss the relationship between the pore network structure and fitted activation energies E_a and E_b. It follows from Refs. 34 and 35 that the characteristic dimension of the NaY zeolite supercage is about 2 nm.[34,35] The pore diameters of samples A and B are almost the same (~ 50 nm), while the chemical treatment of these samples is different. Glass B was obtained from glass A through additional immersion in the KOH solution. Sample C has pores with an average diameter of 300 nm and, as in the case of sample A, was not specially purified with KOH.[32,33]

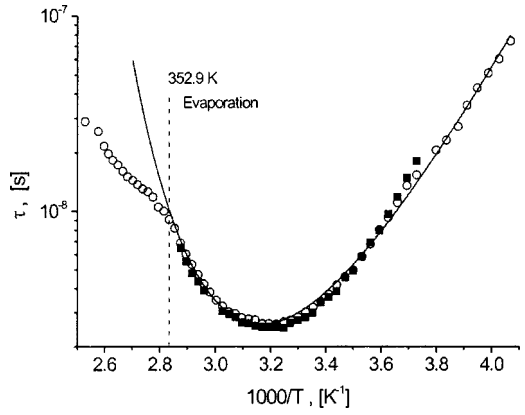

FIG. 2. Temperature dependency of the dielectric relaxation time of water confined in NaY zeolite with faujasite structure. Black squares represent experimental data from Ref. 34. Open cycles correspond to data from Ref. 35. Full line shows the best fit according to Eq. (11); $\ln \tau_0 = -40.1 \pm 0.7$, $E_a = 48 \pm 1$ kJ/mol, $E_b = 25 \pm 1$ kJ/mol, $C = 2.4 \times 10^4 \pm 0.9 \times 10^4$. The dashed line marks the point where the experimental data start to deviate from model (11), most probably, due to the evaporation of water.

It follows from the fit presented in Fig. 1 that E_b energies for all porous glass samples are about the same value of 33 kJ/mol. However, for sample B the value of E_b is about 10% less than those for samples A and C. This fact probably can be explained by the additional chemical treatment of sample B with KOH, which removes the silica gel from the inner surfaces of the pore network. It is reasonable to assume that the defects generally formed at water interfaces and only then penetrated into the water layer. Thus, it seems that the KOH treatment decreases the interaction between the water and inner pore surfaces and consequently decreases the defect formation energy E_b. Following this logic, it can be concluded that in the case of NaY the strength of the interaction between the water molecules and the inner pore surface is even less than this strength for sample B since the defect formation energy E_b for NaY is about 25% less than 33 kJ/mol (see Fig. 2).

This finding is also supported by the specific phenomena observed for NaY in the high temperature range. As can be seen in Fig. 2, there is a significant deviation apart from the model (11) for this sample in the temperature range above 352.9 K. This phenomenon was assigned to the evaporation of water out of the molecular cage of NaY.[35] However, in Fig. 1, there is no sign of a similar process. Thus, this observation once again implies that the interaction between the water molecules and pore interface is significantly less for the NaY zeolite than for the porous glasses A, B, and C.

Dielectric relaxation of confined liquid crystal

The dielectric behavior of liquid crystal 8CB (4-*n*-*octyl*-4′-cyanobiphenyl) has been investigated thoroughly.[43–49] Molecules of 8CB have quite large dipole moments (about 17×10^{-30} C m or 5 D) oriented along the molecule's long axis, making dielectric measurements of this liquid crystal a comparatively simple task. In addition to the nematic phase in the region between 306.7 K and 314 K, bulk 8CB has a smectic-*A* phase in the temperature range from 294.3 K up to 306.7 K. Confined in a nanoporous matrix, 8CB exhibits a rich dielectric spectrum with several separated relaxation processes, which can be ascribed to the MWS interfacial polarization effect, reorientation of 8CB molecules situated at the pore walls, the ''bulklike'' reorientation around the short molecular axis, and the so-called librational (tumbling) mode.[36]

This paper discusses the temperature dependence of the librational mode relaxation time of confined 8CB. In this regard, it is necessary to note that a dielectric spectroscopy investigation of this mode requires the following experimental condition: the probing electrical field should be perpendicular to the direction of the molecular dipole. Therefore, to conduct such a study, the authors of Ref. 36 used the Anopore membrane matrix with cylindrical parallel pores of 200 nm diameter treated with lecithin. This treatment provides a homeotropic boundary condition for 8CB, i.e., all molecules become oriented perpendicular to the pore walls. Thus, by aligning a probing electrical field along the pore axis, the necessary requirements for measuring the librational mode relaxation kinetics are satisfied.

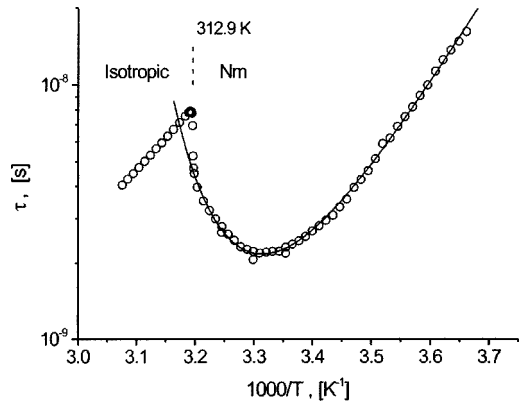

FIG. 3. Temperature dependency of the dielectric relaxation time for the librational mode in the 8CB liquid crystal confined in parallel cylindrical pores Ref. 36. Symbols represent experimental data. Full line corresponds to the best fit according to Eq. (11): $\ln \tau_0 = -49.7 \pm 0.2$, $E_a = E_b = 72.2 \pm 0.4$ kJ/mol, $C = 3.1 \times 10^{12} \pm 0.5 \times 10^{12}$. The vertical dashed line marks the transition between nematic (Nm) and isotropic phases of confined 8CB.

The experimental results in Fig. 3 show well-pronounced nonmonotonic behavior in the low temperature region before the nematic-isotropic transition at 312.9 K, while after the transition this relaxation mode exhibits Arrhenius relaxation kinetics. This transition is also well observed for the reorientation of 8CB molecules around their short axis presented in Fig. 4.

The nonmonotonic behavior of relaxation kinetics for the librational mode in confined 8CB was phenomenologicaly discussed in Ref. 36 as a complex phenomenon, having its origin in two different processes. The authors of Ref. 36 suggested that in the low temperature range, where the relaxation time normally decreases with temperature, relaxation kinetics is mainly governed by the variations of 8CB viscosity. In contrast, at the high temperature range, where the relaxation abnormally increases with temperature, the ordering effect is important. In this region the decrease of the order parameter with temperature increase leads to the growth of amplitude for the molecular orientation fluctuations and this higher amplitude of fluctuations implies longer relaxation times.[36]

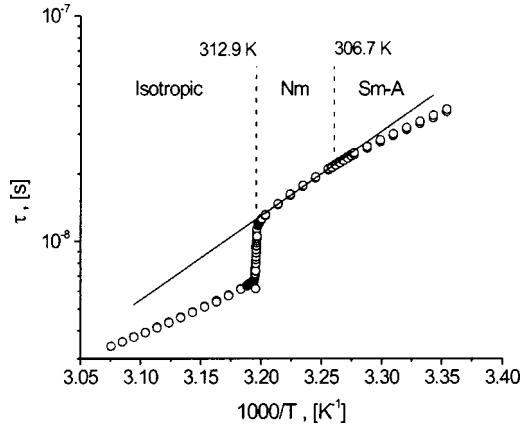

FIG. 4. Temperature dependency of the dielectric relaxation time of the process due to reorientation of molecules around their short axis in confined 8CB (Ref. 36). Symbols represent the experimental data. The full line corresponds to Arrhenius dependence, Eq. (1), in the nematic phase of confined 8CB: $\ln \tau_0 = -45.8 \pm 0.5$, $E_a = 72 \pm 1$ kJ/mol. The vertical dashed lines mark transitions between smectic-*A* (Sm-*A*), nematic (Nm), and isotropic states of 8CB.

In this regard, model (11) suggests an alternative interpretation for the experimental data. As can be seen in Fig. 3, this model reasonably describes the data in the ordered phase excluding the region of the nematic-isotropic phase transition around 312.9 K. The fitting presented in this figure shows that the activation energies, E_a and E_b, for the librational mode in confined 8CB are equal to each other and both are about 72 kJ/mol. Thus, following model (11) paradigm, it can be argued that the librational mode in this case is provided by a single process that is a kind of reorientation or tilt of an 8CB molecule. This tilt, or reorientation, should play a double role in the process under consideration. First, since it is an activated process, it should provide an Arrhenius term in model (11); second, since a tilted molecule may block and open the possibility to tilt for the molecules in its vicinity, it should provide a decrease of the free volume and produce the second exponential term in Eq. (11). Note that activation energies E_a and E_b are quite close to the activation energy of reorientation in an 8CB molecule around its short axis in the nematic phase (see caption to Fig. 4). This coincidence may imply that the reorientation of a molecule around its short axis is the process leading to the abnormal saddlelike relaxation kinetics presented in Fig. 3.

Dielectric relaxation in doped ferroelectric crystal

The doped ferroelectric crystals are intensively studied systems due to their practical importance.[50–56] These crystals are perspective candidates for optoelectronic applications. Motivated by these practical needs, dielectric spectroscopy was used in Ref. 37 to characterize the properties of the KTN ($KTa_{0.65}Nb_{0.35}O_3$) ferroelectric crystal of the perovskite structure doped with Cu with a concentration of about one copper ion per thousand unit cells of KTN.

Due to high symmetry a perovskite unit cell has no dielectric dipole moment in the cubic paraelectric phase. However, in the paraelectric phase, the unit cell of a perovskite has lower symmetry, leading to the existence of a comparatively large elementary dipole associated with a unit cell. For example, the value of such a dipole moment for the $BaTiO_3$ perovskite ferroelectric crystal was estimated as 10×10^{-30} C m or 3 D (see p. 378 in Ref. 51).

Under temperature variations, KTN undergoes three transitions among the phases with rhombohedral, orthorhombic, tetragonal, and cubic unit cells as outlined in Fig. 5.[37,50] In the cubic phase above 295.9 K the crystal exhibits paraelectric properties. Below this temperature, the crystal demonstrates ferroelectric behavior, and both subsequent transitions at 289.2 K and at 230 K are transitions between the different unit cells in the ferroelectric phase.

It was observed[37,55] that copper doping in KTN generates a specific relaxation process that does not exist in nondoped crystals. This process demonstrates nonmonotonic tempera-

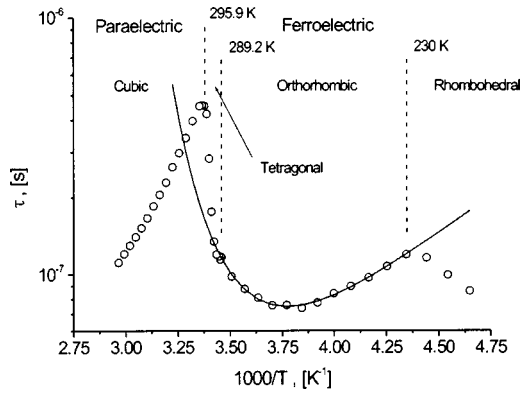

FIG. 5. Temperature dependency of the dielectric relaxation time for the process attributed to Cu doping in KTN. Open cycles represent experimental data from Ref. 37. The full line corresponds to the best fit according to Eq. (11): $\ln \tau_0 = -22 \pm 5$, $E_a = 11 \pm 1$ kJ/mol, $E_b = 33 \pm 4$ kJ/mol, $C = 1.3 \times 10^6 \pm 0..8 \times 10^6$. The dashed lines mark transitions among the phases with rhombohedral, orthorhombic, tetragonal, and cubic unit cells.

ture dependence as presented in Fig 5. It was assumed[37] that this process in the paraelectric phase is due to the reorientation of virtual dipoles provided by the Cu ions hopping between different states of local equilibrium in a multiwell potential created by local fields in the KTN unit cell.

In the ferroelectric phase, this process shows nonmonotonic relaxation kinetics that can be described by model (11) in the temperature range corresponding to the orthorhombic organization of the KTN unit cell (see Fig. 5). In this case, the activation energy $E_b \approx 33$ kJ/mol (see Fig. 5) is similar to that of Cu ion jumps in the multiwell potential in the paraelectric cubic phase of KTN, which is about 38 kJ/mol.[37] Such jumps of Cu ions may create structural ''defects'' in the orthorhombic unit cell. These defects may block and open the possibility of moving some other subunits in the orthorhombic unit cell. Thus, the movements of these subunits should be related to the activation energy E_a.

According to Ref. 37, these mobile subunits are, most probably, the so-called oxygen octahedra, which are six oxygen ion structures situated at the centers of the perovskite unit cell faces. The oxygen octahedron may tilt[57] with respect to the base vectors of the unit cell that leads to the orientation of the elementary dipole moment. The activation energy of this tilt reorientation, evaluated for the similar crystal La_2CuO_4, is about 23 kJ/mol (Ref. 58) and close to the value $E_a \approx 11$ kJ/mol obtained for KTN.

Therefore, it may be argued that the nonmonotonic relaxation kinetics in the ferroelectric orthorhombic phase of KTN is phenomenon dependent on two processes. The first process is the tilt of oxygen octahedron, which changes the orientation of the elementary dipole moments associated with the unit cell and is described by the Arrhenius term with the activation energy E_a in model (11). The second process is Cu ion jumps between the several local minima positions with the activation energy E_b. For the latter process, when a Cu ion reaches a certain place in the multiwell potential, it creates a ''defect'' in the unit cell structure and blocks the possibility for oxygen octahedron to be tilted. Thus, the increase of such ''defects'' with an increase in temperature slows down the relaxation process, as is described by the exponential term in the right-hand side of Eq. (11). In this case, the necessary free volume needed for the oxygen octahedron tilt is provided by the difference in the ionic radii for the Cu^{2+} and K^+ ions while the transition from the paraelectric to ferroelectric phase provides the necessary confinement.[37]

It is also worth looking at here the similarity between the relaxation kinetics patterns presented in Figs. 3 and 5. In both cases, the Arrhenius kinetics appears in disordered homogeneous phases (the isotropic phase of 8CB and the paraelectric phase of KTN), while nonmonotonic relaxation kinetics occurs in the ordered phases (nematic and smectic-*A* phases of 8CB and ferroelectric phases of KTN). This observation highlights the basic idea of model (11): to be valid this model needs not only confinement, but also the possibility of introducing a kind of defect in regular structures. Evidently, this possibility exists only for ordered substances.

Folding kinetics of random heteropolymers and proteins

All examples of nonmonotonic relaxation kinetics discussed above were related to the physical phenomena involving a reorientation of some elementary subunits of a macroscopic system in a confined geometry. However, the nonmonotonic kinetics is also inherent to macromolecular folding.[38–41,59–62]

The macromolecular folding process is a transition from a chainlike macromolecular structure, a so-called unfolded or steric state, to the three-dimensional globular conformation of a macromolecule, the so-called folded state or native conformation in the case of biopolymers.[61] Sometimes the folding process is regarded as a complex chemical reaction and alternatively, as a physical transition. Thus, a number of works argue about this process, using the folding reaction rate k_f description, and, alternatively, some part of the investigators imply the terms of folding times $\tau_f = 1/k_f$. Both descriptions are equivalent from a phenomenological point of view. However, to be consistent with previous examples in our work we shall continue with physical terminology.

Folding is an extremely complex process, especially in the case of biopolymers. Many efforts have been undertaken in order to clarify its nature preceding the pioneering work,[38] which utilized the REM, borrowed from solid state physics[63] to describe protein folding. However, despite the fact that REM significantly advances progress in the scientific understanding of folding, there are still many unsolved problems.[64] Therefore, there is an alternative point of view that treats folding in the framework of the modified theory of transition states.[39]

It has already been mentioned that biopolymer folding is a very complex process in which the internal correlations between different parts of a macromolecule are important. Most probably, this is an asynchronous process in that the correlations may change at different folding stages. In this regard, it should be pointed out that the model (11) does not imply any correlations by virtue of the independent probabilities in Eq. (7).

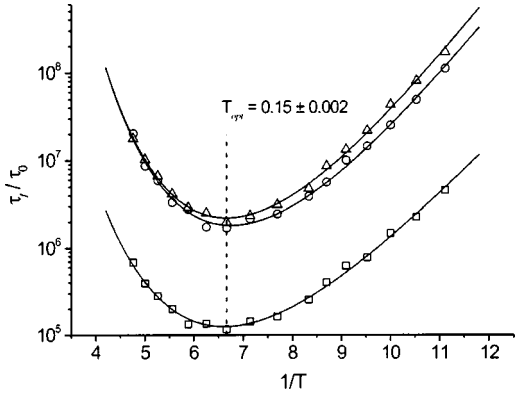

FIG. 6. Temperature dependency of the folding time for three random amino acid sequences of equal length $N=27$ (Refs. 40 and 41). The data in this figure imply that $k_B=1$ and is dimensionless. Symbols represent experimental data. Full lines correspond to the best fit according to Eq. (11). Sequence 1 (cycles): $\ln \tau_0=-1.2 \pm 0.4$, $E_b=0.488\pm0.002$, $q=3.36\pm0.08$, $E_a=q\ E_b=1.637$, $C=qN=90.6$. Sequence 4 (boxes): $\ln \tau_0=1.8\pm0.3$, $E_b=0.498 \pm 0.002$, $q=2.73\pm0.07$, $E_a=q\ E_b=1.362$, $C=qN=73.8$. Sequence 8 (triangles): $\ln \tau_0=-2.1\pm0.3$, $E_b=0.495\pm0.001$, $q=3.40\pm0.06$, $E_a=q\ E_b=1.683$, $C=qN=91.8$. The dashed line marks the temperature T_{opt} corresponding to the fastest folding time τ_{fast}.

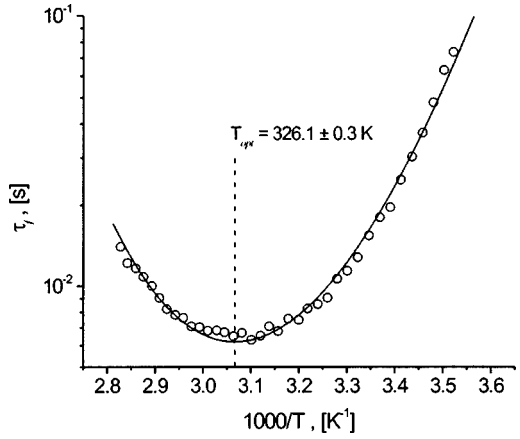

FIG. 7. Temperature dependency of folding time for the CI2 obtained from pH jumps at pH 6.3 (Ref. 39). Symbols represent the experimental data. The full line corresponds to the best fit according to Eq. (11): $\ln \tau_0=-83\pm2$, $E_b=11.28\pm0.01$ kJ/mol, $q=15.1 \pm 0.3$, $E_a=q\ E_b=178.5$, $C=qN=966.5$, $N=64$. The dashed line marks the temperature T_{opt} corresponding to the fastest folding time $\tau_{fast}=6.1$ ms.

The initial simplified example is related to computer simulations of random heteropolymer folding that also does not imply any correlations between the macromolecule constituents. This example will be considered, i.e., the data borrowed from Ref. 40, dealing with simulations of random amino acid sequences via a three-dimensional lattice model.

The computer simulation data from Ref. 40 for three different random sequences of 27 amino acids (sequences 1, 4, and 8) compared with the fitting curves is presented in Fig. 6. As can be seen, model (11) reasonably fits these data. However, there is one important feature in the interpretation of model (11). In contrast to the previous examples, in the case under consideration the confinement does not appears in real space, but does appears in the configurational space of macromolecular conformations.[41] Thus, in the case of folding the probabilities p_1 and p_2 in Eq. (7) should be regarded as the probabilities of breaking a bond between the neighboring beads in a macromolecule chain and the probability of finding the native contact for a certain bond, respectively. Then, in this case is the bond energy of two beads E_b and other parameters of the model (11) obey[41]

$$E_a=qE_b, \quad C=qN, \tag{14}$$

where q is the averaged number of degrees of freedom per bead in the macromolecular chain and N is the number of beads (length of a macromolecule or the number of residues for biopolymer). As can be recognized from the capture for Fig. 6, the fitted values of E_b are almost the same for all analyzed sequences, meaning that for these model systems, it is necessary to expend roughly the same energy to establish a bond between the two beads of the macromolecule chain. Thus, the only parameter that varies the curve shapes is the averaged number of degrees of freedom per bead q.

To test model (11) for folding kinetics of the real biopolymer, the experimental data for CI2 borrowed from Ref. 39, where used. This biopolymer consists of 64 residues and was the first real protein discussed in the framework of two-state mechanism.[65] However, as can be observed in Fig. 7, these experimental data may also be treated in the framework of model (11). The coincidence between the experimental data for real CI2 protein (which certainly has internal correlations between its constituents) and model (11) (which does not imply any correlation) most probably means that the nonmonotonic saddlelike character of the biopolymer folding kinetics is independent of internal correlations.

The above statement is essentially different from the general opinion that internal correlations in macromolecules are responsible for all folding properties. In this regard, Levinthal's famous paradox should be mentioned.[61,66] This claims that the random search through the whole space of protein conformations implies an exponential increase of τ_f with the protein length $\tau_f=\tau_0 q^N$ and leads to the enormously lengthy folding times that cannot explain comparatively the fast folding of real proteins. The usual point of view is that this paradox should be resolved through the concept of internal correlations.[60,61,67,68]

Taking Eq. (14) into account from Eqs. (12) and (13), the following expressions are obtained:

$$T_{opt}=\frac{E_b}{k_B \ln(N)} \tag{15}$$

and

$$\tau_{fast}=\tau_0(e\ \ N)^q \tag{16}$$

Thus, model (11) implies that the fastest folding time τ_{fast}, corresponding to the T_{opt}, demonstrates power-law dependency on macromolecular length that is considerably slower than the exponential growth discussed by Levinthal. It has

already been mentioned that model (11) does not imply any correlation between constituents of a macromolecule, but rather implies a random search for the folded conformation. However, in this case, the idea of confinement provides a significant decrease of searching time due to the decrease of the configurational space.

DISCUSSION

Possible modifications of the model

All the examples described above show that confinement in many cases may be responsible for nonmonotonic relaxation kinetics and could lead to a saddlelike dependence of relaxation time versus temperature. However, this is not the only possible reason for nonmonotonic kinetics. For instance, Ref. 69, devoted to the dielectric study of an antiferromagnetic crystal, discusses a model based on the idea of screening particles. Starting from the Arrhenius equation and implying that the Arrhenius activation energy has linear dependency on the concentration of screening charge carriers, the authors of Ref. 69 also obtained an expression that can lead to the nonmonotonically obtained relaxation kinetics under certain conditions. However, the experimental data discussed in this work do not clearly show a saddlelike behavior of relaxation time temperature dependence. The authors of Ref. 69 do not even discuss such a possibility. Therefore, at the moment it is difficult to judge whether the model in Ref. 69 is relevant to real systems having saddlelike nonmonotonic kinetics.

At the same time, model (11) is also open to modifications. This model is based on assumptions (8) and (9) regarding temperature dependencies for the probabilities p_1 and p_2. Implying a cooperative term of VFT type for p_1, instead of the Arrhenius law (8), we find the temperature dependency of relaxation time is obtained in the form

$$\ln\left(\frac{\tau}{\tau_0}\right)=\frac{DT_K}{T-T_K}+C\exp\left(-\frac{E_b}{k_BT}\right), \tag{17}$$

where the first term of VFT type on the right hand side of Eq. (12) could express the idea of cooperative behavior in accordance with the Adam-Gibbs model.[17]

Confined glassy water

The experimental data for water confined in the porous glass sample C that was discussed in the preceding section (see Fig. 1), is well fitted with Eq. (17) as presented in Fig. 8. Compared to other samples, this porous glass has the largest pore diameter and humidity.[32,33] Therefore, it is reasonable that the cooperative relaxation properties, described by the VFT term, should be more pronounced for this sample. It is worth noting that the fitted value of the Kauzmann temperature $T_K=124\pm7$ K (see caption for Fig. 8). From the T_K value, using the empirical rule $T_g\sim(1.1-1.2)T_K$,[10] the estimation $T_g\sim145$ K of the water-glass transition temperature could be obtained. This value is in fair agreement with usual estimations T_g for water that are expressed by the interval $T_g\approx130\pm6$ K.[70–72] The fitted value of fragility $D=10\pm2$ is close to the estimations of this parameter $D\approx8$ that have been derived from the diffusivity data for the amorphous solid water in Ref. 71. These findings may also support the idea that the porous glass samples treated in the preceding discussion dealt with a kind of noncrystalline state of water. The most probable reason for this is the pore walls providing the necessary confinement. Note that in porous glasses the glassy properties of water can be observed at the comparatively high temperatures about room temperature, whereas the usual ways to obtain glassy water require quite low temperatures and special treatment.[70,71] However, to support these experimental findings further instigations are required.

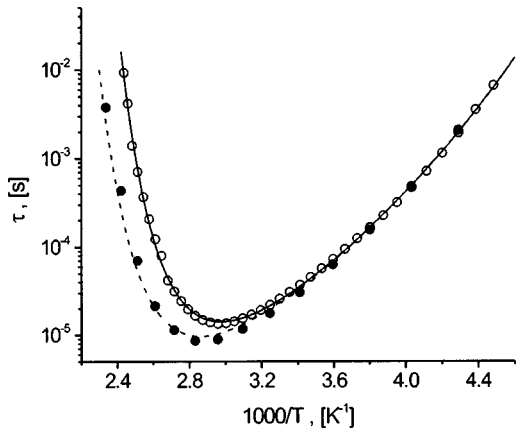

FIG. 8. Temperature dependency of dielectric relaxation time for water confined in sample C. The data were measured under different conditions and contain a different amount of water: open circles correspond to the data presented earlier in Fig. 1; full circles represent the experiment with reduced water content (Ref. 73). Full line is the best fit according to Eq. (17): $\ln\tau_0=-17.8\pm0.5$, $E_b=39\pm1$ kJ/mol, $T_K=124\pm7$ K, $D=10\pm2$, $C=9\times10^5\pm3\times10^5$. The dashed line was simulated from Eq. (17) for the same $\ln\tau_0$, E_b, T_K and D, but with C divided by a factor 1.8 (see explanation in text).

Relationships between the static properties and dynamics

The next idea is to compare the data obtained from the kinetics and other relaxation process parameters. The data for water confined in porous glass C could be discussed in relation to the kinetics and static properties of the dielectric relaxation processes related to the two different experiments.[73] The two experimental runs presented in Fig. 8 are quite similar at the low temperatures. However, in the high temperature range, they exhibit a remarkable difference from each other.

In Fig. 9, temperature dependencies of the so-called dielectric strength $\Delta\varepsilon$ for these experiments are presented. The dielectric strength is the difference between high and low frequency limits of the real part of the complex dielectric permittivity of the process under consideration. This quantity reflects the concentration of dipole moments n_d in a sample and, in its simplest approximation, is in linear proportion to concentration $\Delta\varepsilon\sim n_d$,[74] i.e., the dielectric strength is proportional to the water content. Thus, the two experimental runs presented in Fig. 9, as well as data in Fig. 8, correspond to the two different amounts of water in sample C.

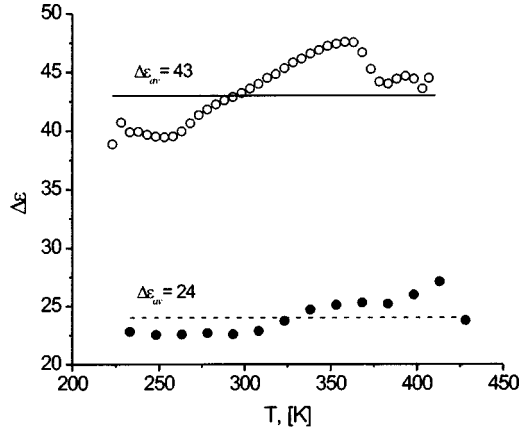

FIG. 9. Temperature dependence of the dielectric strength $\Delta\varepsilon$ for sample C. Symbols represent experimental data corresponding to the relaxation times presented in Fig. 8: open circles correspond to the data presented earlier in Fig. 1; full circles represent the experiment with reduced water content (Ref. 73). The lines mark values of the averaged dielectric strength $\Delta\varepsilon_{av}$ for these experiments.

Recall that the preexponential factor $C=v_0 n_0/V$, where n_0 is the maximum possible number of defects. This number is proportional to the water content and $C\sim n_0\sim n_d\sim\Delta\varepsilon$. The dielectric strength $\Delta\varepsilon$ for these runs are almost constant (the variations of $\Delta\varepsilon$ are about 5% of the averaged value for both runs). By comparing the averaged values of $\Delta\varepsilon$ for these runs, the difference in water content between these experiments has been estimated to be 1.8 times (see Fig. 9). The preexponential factors C for these two situations should also be different by the same factor. The comparison in Fig. 8 shows that this is actually so.

CONCLUDING REMARK

The main goal of our paper was the idea that confinement could be responsible for the nonmonotonic relaxation kinetics and could provide a specific saddlelike temperature dependency for relaxation time. The experimental examples discussed show that this type of kinetics may be inherent to the systems of absolutely different natures: confined liquids, ferroelectric and liquid crystals, and even macromolecular folding kinetics. In these cases, the particular interpretation of the parameters of model (11) is dependent on the discussed experimental situation. We are far from the opinion that confinement is the only reason for nonmonotonic relaxation kinetics. However, for all the examples discussed in this paper, the nonmonotonic dependence of the relaxation time on temperature has the same origin, that is, confinement either in real or configurational space.

ACKNOWLEDGMENTS

The authors wish to express their deep gratitude to Professor F. Aliev for the kind opportunity to use his experimental data and acknowledge his important notes about 8CB relaxation dynamics. We also appreciate the help received from Professor. A. Schönhals, who provided us with the experimental data on dielectric relaxation of water in NaY zeolite. Furthermore, we gratefully acknowledge the help of Mrs. A. Gutina with the data treatment. And one of us (Ya. R.) expresses his deep gratitude to The Hebrew University of Jerusalem for its hospitality.

*Author to whom correspondence should be addressed. Email address: yurif@vms.huji.ac.il

[1] S. Arrhenius, Z. Phys. Chem., Stoechiom. Verwandtschaftsl. **4**, 226 (1889).
[2] H. Eyring, Chem. Rev. (Washington, D.C.) **17**, 65 (1935).
[3] H. Eyring, J. Chem. Phys. **3**, 107 (1935).
[4] H. Eyring, Trans. Faraday Soc. **34**, 41 (1938).
[5] C. J. F. Böttcher and P. Bordewijk, *Theory of Electric Polarization*, 2nd ed. (Elsevier, Amsterdam, 1992), Vol. 2.
[6] D. Eisenberg and W. Kauzmann, *The Structure and Properties of Water* (Clarendon, Oxford, 1969).
[7] J. Barthel, R. Buchner, and B. Wurm, J. Mol. Liq. **98–99**, 51 (2002).
[8] R. Buchner and J. Barthel, Chem. Phys. Lett. **306**, 57 (1999).
[9] C. A. Angell, J. Non-Cryst. Solids **73**, 1 (1985).
[10] C. A. Angell, J. Non-Cryst. Solids **131–133**, 13 (1991).
[11] R. Böhmer, K. L. Ngai, C. A. Angell, and D. J. Plazek, J. Chem. Phys. **99**, 4201 (1993).
[12] R. Richert, C. A. Angell, J. Chem. Phys. **108**, 9016 (1998).
[13] R. Brand, P. Lunkenheimer, and A. Loidl, J. Chem. Phys. **116**, 10 386 (2002).
[14] H. Vogel, Phys. Z. **22**, 645 (1921).
[15] G. S. Fulcher, J. Am. Ceram. Soc. **8**, 339 (1925).
[16] G. Tammann and W. Hesse, Z. Anorg. Allg. Chem. **156**, 245 (1926).
[17] G. Adam and J. H. Gibbs, J. Chem. Phys. **43**, 139 (1965).
[18] W. Kauzmann, Chem. Rev. (Washington, D.C.) **43**, 219 (1948).
[19] T. G. Fox and P. J. Flory, J. Appl. Phys. **21**, 581 (1950).
[20] T. G. Fox and P. J. Flory, J. Physiol. (London) **55**, 221 (1951).
[21] T. G. Fox and P. J. Flory, J. Polym. Sci. **14**, 315 (1954).
[22] A. K. Doolittle, J. Appl. Phys. **22**, 1471 (1951).
[23] D. Turnbull and M. H. Cohen, J. Chem. Phys. **34**, 120 (1960).
[24] J. T. Bendler and M. F. Shlesinger, J. Mol. Liq. **36**, 37 (1987).
[25] J. T. Bendler and M. F. Shlesinger, J. Stat. Phys. **53**, 531 (1988).
[26] J. T. Bendler, J. J. Fontanella, and M. F. Shlesinger, Phys. Rev. Lett. **87**, 195503 (2001).
[27] W. Götze, in *Freezing and Glass Transition*, Les Houches Session LI, edited by D. Levesque, J. Zinn-Justin and J. P. Hasen (North-Holland, Amsterdam, 1991) p. 289; W. Götze and L. Sjögren, Rep. Prog. Phys. **55**, 241 (1992).
[28] U. Bengtzelius, W. Götze, and A. Sjölander, J. Phys. C **17**, 5915 (1984).
[29] P. Taborek, R. N. Kleiman, and D. J. Bishop, Phys. Rev. B **34**, 1835 (1986).
[30] R. Richert and H. Bässler, J. Phys.: Condens. Matter **2**, 2273 (1990).
[31] J. Schüller, R. Richert, and E. W. Fischer, Phys. Rev. B **52**, 15 232 (1995).
[32] A. Gutina, E. Axelrod, A. Puzenko, E. Rysiakiewicz-Pasek, N. Kozlovich, Y. Feldman, J. Non-Cryst. Solids **235–237**, 302 (1998).

[33] Ya. Ryabov, A. Gutina, V. Arkhipov, and Yu. Feldman, J. Phys. Chem. B **105**, 1845 (2001).
[34] L. Frunza, H. Kosslick, S. Frunza, R. Fricke, and A. Schönhals, J. Non-Cryst. Solids **307–310**, 503 (2002).
[35] L. Frunza, H. Kosslick, S. Frunza, R. Fricke, and A. Schönhals, J. Phys. Chem. B **106**, 9191 (2002).
[36] F. M. Aliev, Z. Nazario, and G. P. Sinha, J. Non-Cryst. Solids **305**, 218 (2002).
[37] P. Ben Ishai, Ya. Ryabov, Yu. Feldman, and A. Agranat (unpublished).
[38] J. D. Bryngelson and P. G. Wolynes, Proc. Natl. Acad. Sci. U.S.A. **84**, 17 524 (1987).
[39] Y.-J. Tan, M. Oliveberg, and A. R. Fersht, J. Mol. Biol. **264**, 377 (1996).
[40] A. Gutin, A. Sali, V. Abkevich, M. Karplus, and E. I. Shaknovich, J. Chem. Phys. **108**, 6466 (1998).
[41] Ya. Ryabov, J. Phys. Chem. B **107**, 12009 (2003).
[42] V. F. Petrenko and R. W. Whitworth, *Physics of Ice* (Oxford University Press, Oxford, 1999).
[43] P. G. Cummins, D. A. Danmur, and D. A. Laidler, Mol. Cryst. Liq. Cryst. **30**, 109 (1975).
[44] D. Lippens, J. P. Parneix, and A. Chapoton, J. Phys. (France) **38**, 1465 (1977).
[45] J. M. Wacrenier, C. Druon, and D. Lippens, Mol. Phys. **43**, 97 (1981).
[46] T. K. Bose, R. Chahine, M. Merabet, and J. Thoen, J. Phys. (France) **45**, 11 329 (1984).
[47] A. Buka and A. H. Price, Mol. Cryst. Liq. Cryst. **116**, 187 (1985).
[48] T. K. Bose, B. Campbell, S. Yagihara, and J. Thoen, Phys. Rev. A **36**, 5767 (1987).
[49] H. G. Kreul, S. Urban, and A. Würtfinger, Phys. Rev. A **45**, 8624 (1992).
[50] S. Triebwasser, Phys. Rev. **114**, 63 (1959).
[51] C. Kittel, *Introduction to the Solid State Physics*, 6th ed. (Wiley, New York, 1986).
[52] A. Bussmann-Holder, H. Bliz, and G. Benedek, Phys. Rev. B **39**, 9214 (1989).
[53] B. E. Vugmeister and D. Glinchuk, Rev. Mod. Phys. **62**, 993 (1990).
[54] C.-S. Tu, I. G. Siny, and V. H. Schmidt, Phys. Rev. B **49**, 11 550 (1994).
[55] G. Bitton, Yu. Feldman, and A. J. Agranat, J. Non-Cryst. Solids **305**, 362 (2002).
[56] V. A. Trepakov, L. Jastrabik, S. Kapphan, E. Giulotto, and A. Agranat, Opt. Mater. (Amsterdam, Neth.) **19**, 13 (2002).
[57] A. M. Glazer, Acta Crystallogr., Sect. B: Struct. Crystallogr. Cryst. Chem. **28**, 3384 (1972).
[58] F. Cordero, A. Campana, M. Corti, A. Rigamonti, R. Cantelli, and M. Ferretti, Int. J. Mod. Phys. B **13**, 1079 (1999).
[59] C. B. Anfinsen, E. Haber, M. Sela, and F. H. White, Proc. Natl. Acad. Sci. U.S.A. **47**, 1309 (1961).
[60] J. D. Bryngelson, J. N. Onuchic, N. D. Socci, and P. G. Wolynes, Proteins: Struct., Funct., Genet. **21**, 167 (1995).
[61] L. Stryer, *Biochemistry*, 4th ed. (Freeman, New York, 1995).
[62] T. Schindler and F. X. Schmid, Biochemistry **35**, 16 833 (1996).
[63] B. Derrida, Phys. Rev. Lett. **45**, 79 (1980).
[64] V. S. Pande, A. Yu. Grosberg, C. Joerg, and T. Tanaka, Phys. Rev. Lett. **77**, 5433 (1996).
[65] D. E. Otzen, L. S. Itzhaki, N. F. ElMasry, S. E. Jackson, and A. R. Fersht, Proc. Natl. Acad. Sci. U.S.A. **91**, 10 422 (1994).
[66] C. Levinthal, in *Mossbauer Spectroscopy in Biological Systems*, Proceedings of a meeting held at Allerton house, Monticello, IL, edited by J. DeBrunner, J. C. M. Tsibris, and E. Münck (University of Illinois Press, Urbana, 1969) pp. 22–24.
[67] A. V. Finkelstein, J. Biomol. Struct. Dyn. **20**, 311 (2002).
[68] A. Grosberg, J. Biomol. Struct. Dyn. **20**, 317 (2002).
[69] A. A. Bokov, M. Mahesh Kumar, Z. Xu, and Z.-G. Ye, Phys. Rev. B **64**, 224101 (2001).
[70] G. P. Johari, A. Hallbruker, and E. Mayer, Nature (London) **330**, 552 (1987).
[71] R. S. Smith and B. D. Kay, Nature (London) **398**, 788 (1999).
[72] B. Bergman and J. Swenson, Nature (London) **403**, 283 (2000).
[73] A. Gutina and Yu. Feldman (unpublished). These data were measured at the same time as the data presented in Refs. 32 and 33. However, they were not included in the discussion due to the lack of interpretation at that time.
[74] H. Fröhlich, *Theory of Dielectrics* (Clarendon, Oxford, 1958).